HHS Public Access

Author manuscript

Cancer Prev Res (Phila). Author manuscript; available in PMC 2016 August 01.

Published in final edited form as:

Cancer Prev Res (Phila). 2015 August ; 8(8): 720–728. doi:10.1158/1940-6207.CAPR-14-0407.

Activation of the PI3K/Akt/mTOR and MAP kinase Signaling Pathways in Response to Acute Solar Simulated Light Exposure of Human Skin

Yira Bermudez[1,2], **Steven P. Stratton**[1,2], **Clara Curiel-Lewandrowski**[1,2], **James Warneke**[1,2,3], **Chengcheng Hu**[2], **George T. Bowden**[2], **Sally E. Dickinson**[2], **Zigang Dong**[4], **Ann M. Bode**[4], **Kathylynn Saboda**[2], **Christine A. Brooks**[2], **Emanuel F. Petricoin III**[5], **Craig A. Hurst**[1,3], **David S. Alberts**[1,2], and **Janine G. Einspahr**[1,2]

[1]College of Medicine, University of Arizona, Tucson, Arizona 85724

[2]The University of Arizona Cancer Center, Tucson, Arizona 85724

[3]Department of Surgery, University of Arizona, Tucson, Arizona 85724

[4]The Hormel Institute, University of Minnesota, Austin, Minnesota 55912

[5]George Mason University, Manassas, Virginia 20110

Abstract

The incidence of skin cancer is higher than all other cancers and continues to increase, with an average annual cost over $8B in the United States. As a result, identifying molecular pathway alterations that occur with UV exposure to strategize more effective preventive and therapeutic approaches is essential. To that end, we evaluated phosphorylation of proteins within the PI3K/Akt and MAPK pathways by immunohistochemistry in sun-protected skin after acute doses of physiologically relevant solar simulated ultraviolet light (SSL) in 24 volunteers. Biopsies were performed at baseline, 5-minute, 1-, 5-, and 24-hour post SSL. Within the PI3K/Akt pathway, we found activation of Akt (Serine473) to be significantly increased at 5 hrs while mTOR (Serine2448) was strongly activated early and was sustained over 24-hour post SSL. Downstream we observed a marked and sustained increase in phospho-S6 (Serine235/S236) whereas phospho-4E-BP1 (Threonines37/46) was increased only at 24 hours. Within the MAPK pathway, SSL-induced expression of phospho-p38 (Threonine180/Tyrosine182) peaked at 1–5 hrs. ERK 1/2 was observed to be immediate and sustained post-SSL. Phosphorylation of histone H3 (Serine10), a core structural protein of the nucleosome, peaked at 5-hour post SSL. The expression of both p53 and COX-2 was increased at 5-hour and was maximal at 24-hour post SSL. Apoptosis was significantly increased at 24 hrs as expected and indicative of a sunburn-type response to SSL. Understanding the timing of key protein expression changes in response to SSL will aid in development of mechanistic-based approaches for the prevention and control of skin cancers.

Corresponding Author. Janine G. Einspahr, The University of Arizona Cancer Center, 1515 N. Campbell Ave, P.O. Box 245024, Tucson, AZ 85724. Phone: 520-626-2444. Fax: 520-626-9275. einspahr@email.arizona.edu.

Disclosure. Clara Curiel-Lewandrowski: MelaSciences, Inc-Consulting; Medical Directions, Inc-Consulting; DermSpectra LLC-Founder/Member

Keywords

mTOR; 4E-BP1; MAPK; cutaneous squamous cell carcinoma; UV-irradiation

Introduction

An estimated 3 million nonmelanoma skin cancer (NMSC) cases are diagnosed in the United States yearly with an estimated 4% yearly increase in the Medicare population (1). Cancer registries do not require NMSCs to be reported, and as such, precise estimations of NMSC numbers are problematic. Approximately 75–80% of NMSCs diagnoses are basal cell carcinomas (BCC) and 18% are squamous cell carcinomas (SCC). This high incidence of skin cancer is directly related to chronic solar radiation exposure (2). SCCs result from the malignant transformation and proliferation of squamous cells, the most abundant cell in the epidermis. Although NMSCs have a fairly low metastatic potential, the morbidity associated with NMSCs is high and available treatments can be disfiguring as well as expensive (3). In Medicare recipients over the age of 65, approved physician charges for treatment of NMSC totaled at least $285 million per year in 2001, while 2011 estimates indicate an annual cost in both Medicare and non-Medicare populations at over $8 billion (3, 4). This striking massive increase in treatment costs further illustrates the growing problem of skin cancer. Current primary skin cancer prevention strategies, including sun avoidance and ultraviolet (UV) protection, have had limited success (5). Therefore, a need exists for new mechanism-based approaches to prevent and treat solar radiation-induced skin cancers. To that end, determining the effect of solar radiation on skin in both the acute and chronic settings is essential.

UV radiation has been shown to be a complete carcinogen by way of mutations, many of which are signature UV mutations, in the DNA of critical genes. Additionally, UV can act as a promoter through the activation of signal transduction pathways (6). The UV spectrum that reaches the earth’s surface is made up of approximately 95% UVA (320–400 nm) and approximately 5% UVB (280–320 nm) (7). The majority of studies on the role of UV in activation of signaling pathways and skin carcinogenesis have focused on UVA (8, 9) or UVB (10–12) alone, and in some cases UVC, which does not reach the earth’s surface in appreciable amounts (13). Fewer studies have focused on the entire spectra of UVA and UVB combined in a ratio that mimics the solar spectrum (13). Strong experimental evidence indicates that exposure of epidermal cells to UV results in the activation of numerous signal transduction pathways that include the PI3K/Akt and MAPK cascades (7).

The phosphoinositide-3-kinase/protein kinase B (PI3K/Akt) pathway is an effector of cell survival and proliferation (14). Stimulation of the PI3K/Akt pathway results in the activation of downstream kinases that include mammalian target of rapamycin (mTOR), p70 ribosomal protein S6 kinase 1 (p70S6K1) and 4E-binding protein 1 (4E-BP1). Phosphorylation of 4E-BP1 by mTOR inhibits its activity, which in turn, leads to the activation of cellular translational machinery through inhibition of eIF4E by phosphorylated 4E-BP1. Inhibition of 4E-BP1 results in the inhibition of eIF4E, which ultimately results in the activation of translation machinery. Also, mTOR can directly activate p70S6K1, which can then activate

a downstream target, ribosomal protein S6 (S6), leading to the initiation of protein synthesis (15). Studies have shown that mTOR is activated by UVB, and further; aberrant activation of the mTOR pathway has been implicated in the development of SCC (6, 16). mTOR is known to coordinate cell cycle progression, cell survival, and growth in response to genetic, epigenetic and environmental conditions including UV-mediated cellular stress (17).

Signaling cascades that lead to activation of mitogen-activated protein kinases (MAPKs) are also important in UV-induced cutaneous SCC (18), particularly, extracellular signal-regulated kinases 1 and 2 (ERK 1/2), c-Jun N-terminal kinases (JNKs) and p38 (12, 13). The MAPK signaling pathways are activated by growth factors and stress stimuli and they play central a role in transducing extracellular signals to target proteins involved in cell growth and proliferation (19, 20). Activated B-Raf phosphorylates and activates ERK 1/2, which in turn phosphorylates several substrates including members of the 90 kDa ribosomal S6 kinase (RS6K) (19, 20). These signaling pathways are regulated by a complex network that includes crosstalk and feedback mechanisms.

The objective of this study was is to determine whether acute doses of solar light (using a solar simulator to generate a measured erythemal dose of solar-simulated light [SSL]) would activate the expression of key proteins/phosphoproteins within the PI3K/Akt/mTOR and MAPK signaling pathways in normally sun-protected skin of healthy volunteers.

Materials and Methods

Study population

Study participants were recruited from a pool of subjects who had been previously screened and/or participated in previous skin chemoprevention trials and had agreed to be re-contacted for future studies. The eligibility criteria for participants from this pool included age of 18 years or older and Fitzpatrick skin types II (burns easily, tans poorly) or III (burns moderately, tans gradually). Exclusion criteria included immunosuppression, serious concurrent illness, invasive cancer (including any type of skin cancer) within the past 5 years and baseline serum chemistry values outside of normal limits. In addition, those using photosensitizing medications or topical medications on the test area during the past 30 days were ineligible. Individuals taking mega doses of vitamins were not eligible (i.e. more than five times the RDA, more than five capsules of multivitamins, 400 IU of vitamin E, 200 g of selenium and 1 g of vitamin C). Additional exclusion criteria included individuals with a history of sun exposure to the buttocks within 30 days of randomization and participants must have agreed to avoid sun exposure during the study period. Finally, individuals with a known allergy to lidocaine were ineligible. The University of Arizona Institutional Review Board approved the study and written informed consent was obtained from all study participants.

Minimal erythema dose (MED)

The minimal erythema dose (MED) of SSL was determined for each individual using a Multiport UV Solar Simulator Model 600 (Solar Light Co., Philadelphia, PA). The spectrum of light generated by the Solar Simulator consisted of 8.7% UVB and 91.3% UVA (21). The

dose of emission was precisely regulated to include the UVA and UVB range (290–390 nm). MED was defined as the smallest dose of energy necessary to produce confluent erythema with distinct borders at 22–26 hours post exposure. MED was determined on a buttock area normally protected from sunlight. Each test area was subdivided into six subsites (each 1 cm^2) corresponding to the liquid light guide pattern on the solar simulator. The solar simulator was calibrated prior to each use and a series of six increasing SSL radiation exposures were administered concurrently at each site area. Following exposure, the test sites were covered until evaluations were completed (22–26 hrs).

Administration of 2–3 MED

After determination of the MED for each individual, the contralateral buttock was exposed to one of the following- 2, 2.5, or 3 times the MED. A 6 mm skin punch biopsy was collected from one buttock at baseline prior to SSL exposure and additional 6 mm punch biopsies were removed at 5 minutes, 1, 5, and 24 hrs post-SSL irradiation. Biopsy sites were then sutured and subjects returned to the clinic for suture removal in approximately 1 week. A dose of 2 MED of SSL was applied to sun-protected skin of 12 subjects. Two additional groups of 6 subjects each received doses of 2.5 and 3 MED SSL.

Immunohistochemistry (IHC)

Biopsies were immediately fixed in 10% neutral buffered formalin for 24 hrs then transferred to 70% ethanol prior to routine processing and paraffin embedding. Tissue sections (5 microns) were deparaffinized and rehydrated. All tissue sections were subjected to antigen retrieval using Diva buffer in a Decloaking Chamber Pro (Biocare, Walnut Creek, CA) for 30 seconds. Immunohistochemical staining was performed using a Vectastain avidin biotin based peroxidase kit with a Novared substrate (Vector Laboratories, Burlingame, CA, PK-6100 and SK-4800) or a Vectastain ABC-AP kit and a Vector red alkaline phosphatase substrate (AK-5000 and SK-5100) depending on the antibody, and a hematoxylin counterstain (Leica Microsystems, Inc., Buffalo Grove, IL). Positive and negative controls were included for each antibody. Antibodies included those to detect phospho-Akt (p-Akt Serine 473, #3787) at 1:100 overnight, p-mTOR (Serine 2448, #2976) at 1:300 overnight, p-4E-BP1 (Threonine 37/46, #2855) at 1:100 overnight, phosphorylated S6 protein (Serine 235/236, #2211) at 1:200 overnight, p-p38 (Threonine 180/Tyrosine 182, #4511) at 1:800 for 1 hour, p-ERK 1/2 (Threonine 202/Tyrosine 204, #4376) at 1:100 overnight, p-histone H3 (Serine 10, #9701) at 1:100 overnight, and cleaved caspase 3 (#9661) at 1:1000 overnight and all purchased from Cell Signaling Technology, Beverly, MA. Antibodies to detect p53 (#OP43) at 1:100 for 1 hour and PCNA at 1:800 for 1 hour were obtained from EMD Chemicals, Inc. (San Diego, CA, #NA03). The antibody to detect COX-2 at 1:100 for 1 hour was from Cayman Chemical (Ann Arbor, MI, #160112).

IHC-stained tissue sections were measured using the ImagePro Plus (Media Cybernetics, Silver Springs, MD) software system, a Leica DMR microscope (Westzlar, Germany), and a Sony 3CCD color video camera (Japan). The mean positive nuclear or cytoplasmic area per 40X field was determined for each biopsy. The number of apoptotic cells was assessed based on morphology (i.e. condensed and/or pyknotic nuclei, eosinophilic cytoplasm,

formation of apoptotic bodies) per 100 basal keratinocytes on hematoxylin & eosin (H&E) stained sections.

Statistical analysis

The percent positive area was calculated for each marker with the exception of the apoptotic markers (cleaved caspase 3 and morphologic apoptosis). Apoptosis was expressed as the number per 100 basal keratinocytes. As seen in Table 1, mean and standard errors were used to describe the data at each time point, where the clustered robust standard error was used in order to adjust for possible correlation of multiple measurements per study participant. The primary research question was to compare the expression level of each IHC marker between baseline and at each of the four time points after SSL exposure. Distribution of the level of each marker was checked graphically and the appropriate transformation, if needed, was applied to achieve approximate normality. The comparison of each maker (possibly after transformation) was performed using the generalized estimating equations (GEE) models, which adjusted for any potential correlation between multiple measurements of the same study subject. For any marker where no appropriate transformation is available to remove heavy skewness the rank was used as the response variable of the GEE models. The three MED groups were adjusted for in the models as confounders. The change in each IHC marker was also compared between the three MED groups using a Wald test based on fitted GEE models (data presented in Supplementary Data). GEE models were also used to conduct a test for trend across the five time points, with adjustment for MED levels. All analyses were conducted using Stata version 13 (Stata Corporation, College Station, TX). All reported p-values were not adjusted for multiple comparisons.

Results

The study included 12 males and 12 females with an average age of 68.3 ± 9.4 (mean ± standard deviation) years for males and 61.1 ± 8.1 years for females. Eighty-three percent (20/24) of the subjects listed themselves as Caucasian, 12.5% (3/24) listed themselves as having more than one race, and 1.7% (1/24) as other. Forty-two percent (10/24) of the subjects had Fitzpatrick skin Type II and 58% (14/24) skin Type III. The solar simulator provided 8.7% of UVB and 91.3% of UVA (21). The aim of the study was to expose subjects to low dose SSL. To that end, 12 participants were exposed to 2 MED with an average (± standard error) dose of 3.6 ± 0.5 J/cm^2 UVA and 51.6 ± 7.0 mJ/cm^2 UVB. After the initial group of 12 subjects the study was expanded to add 2.5 and a 3 MED exposures. Six participants were exposed to 2.5 MED with an average dose of 4.8 ± 0.5 J/cm^2 UVA and 70.0 ± 6.8 mJ/cm^2 UVB and 6 participants were exposed to 3 MED with an average dose of 5.6 ± 0.8 J/cm^2 UVA and 81.4 ± 11.9 mJ/cm^2 UVB. Our primary question was to determine whether there was modulation of key proteins/phosphoproteins within the PI3K/Akt/mTOR and MAPK signaling pathways after SSL, not to compare MED levels. The comparison of protein expression by MED level is presented as Supplementary Figures S1–3. In order to account for the 3 MED levels, statistical models adjusted for MED level as a confounder.

Study results are summarized in Table 1, which shows the mean ± standard error (SE) for each marker and for each time point. As noted earlier, biomarker expression was averaged

over all subjects (12 subjects at 2 MED, 6 at 2.5 MED, and 6 at 3 MED). In Table 1, data are expressed as the percent positive area for all markers with the exception of apoptosis and cleaved caspase 3, which are expressed as the number of apoptotic cells per 100 basal cells. Representative IHC stained micrographs of each biomarker are shown in Figures 1–5. We previously reported that in human sun-protected skin, 4 MED of UV resulted in the phosphorylation of MAPKAPK2, CREB, c-JUN, p38, GSK-3b and p53 leading to markedly increased levels of c-FOS, COX-2 and apoptosis in the epidermal cells (12). In the current study, we investigated the impact of a lower dose of SSL on key proteins within the PI3K/Akt and MAPK pathways by immunohistochemistry. We found that a single dose of 2–3 MED of SSL activated the PI3K/Akt signaling pathway with a small but statistically significant increase in cytoplasmic and nuclear staining of p-Akt at serine 473 (Figures 1a–d, 1.4-fold increase at 5 hrs post SSL; $p=0.01$). We next evaluated mTOR, a direct substrate of activated Akt, for phosphorylation at serine 2448. P-mTOR was present in both the cytoplasm and nucleus of epidermal cells (Figures 1e–h) and its expression was significantly increased from 1 to 24 hrs (1.7-fold; $p=0.02$, 2.2-fold; $p<0.001$, and 3.2-fold; $p<0.001$ at 1, 5, and 24 hrs, respectively). Another PI3K/Akt signaling protein that is downstream of both mTOR and p70S6K1 is S6. We found that p-S6 at serines 235 and 236 showed both cytoplasmic and nuclear staining (Figures 2a–d) and its expression was significantly increased from 1 to 24 hrs (2.9-fold; $p<0.001$, 7.3-fold; $p<0.001$,10.3-fold; $p<0.001$ at 1, 5, and 24 hrs, respectively). We then examined p-4E-BP1 (threonines 37/46), a downstream target of activated mTOR, and found statistically significant increased primarily nuclear immunostaining (Figures 2e–h) at 24 hrs (2.1-fold; $p<0.001$).

We next explored the effect of 2–3 MEDs of SSL on the MAPK signaling pathway. To that end, we examined p38 for dual phosphorylation at threonine 180 and tyrosine 182 and found predominately nuclear expression (Figures 3a–d) from 1 to 24 hrs (2.6-fold; $p<0.001$, 2.7-fold; $p<0.001$, and 2.1-fold; $p<0.001$ at 1, 5, and 24 hrs post SSL, respectively). Another key MAPK pathway protein, ERK1/2, was evaluated for dual phosphorylation on threonine 202 and tyrosine 204. Nuclear expression of p-ERK 1/2 (Figures 2d–h) was presented early (1.4-fold at 5 mins; $p=0.012$) and increased from 1 through 24 hrs (3.9-fold; $p=0.004$ at 1 hr, 5.2-fold at 5 hrs; $p<0.001$, and 5.6-fold at 24 hrs; $p<0.001$). Subsequently, we found that nuclear expression of p-histone H3 at serine 10 (Figures 2i–l) was significantly increased from 1 to 24 hrs with a peak at 5 hrs (5.6-fold; $p<0.001$ at 1 hour, 19.7-fold; $p<0.001$ at 5 hrs, and 6.1-fold; $p<0.001$ at 24 hrs).

In our evaluation of downstream events, we next assessed expression of COX-2, p53, PCNA, cleaved caspase 3, and morphologic apoptosis on H&E. Cytoplasmic expression of COX-2 (Figures 4a–d) was negligible at baseline but was significantly increased starting at 5 hrs (2.3-fold; $p<0.001$) and was maximal at 24 hrs (13.9-fold; $p<0.001$) post SSL with expression primarily in the basal layer. Statistically significant total p53 nuclear expression (Figures 4e–h) was observed beginning at 5 hrs (3.4-fold; $p<0.001$) and was maximal at 24 hrs (20.1-fold; $p<0.001$) post SSL.

As shown in Figures 5a–d, PCNA expression yielded little change over time post SSL with the exception of a small decrease at 5 minutes post SSL ($p=0.023$). Apoptosis was measured by two methods, which included cleaved caspase 3 and a count of morphologically apoptotic

cells (sunburn cells) as observed by H&E. The number of cleaved caspase 3 positive cells (Figures 5e and f) was significantly increased (5-fold; $p<0.001$) at 24 hrs post SSL. The number of morphologically apoptotic cells as visualized by H&E (Figure 5g and h) showed a statistically significant 10.3-fold ($p<0.001$) increase at 24 hrs post SSL.

Analysis of the effect of MED on biomarker expression is shown in Supplementary Figures S1–3. There was not a statistically significant difference in expression of p-Akt (Figure 1a), p-mTOR (Figure 1b), p-4E-BP1 (Figure 1d), p-p38 (Figure 2a), COX-2 (Figure 2d), p53 (Figure 3a), or morphological apoptosis (Figure 3c) by MED level. For p-S6, there was a statistically significant difference (Figure 1c, $p<0.001$) between the three MED levels. The three SSL levels followed the same pattern over time (baseline, 1, 5, and 24 hrs) but the 2 MED dose showed overall higher p-S6 expression. This was also the case for pERK 1/2 (Figure 2b, $p=0.009$) and p-histone H3 (Figure 2c, $p=0.007$). In the case of cleaved caspase 3 (Figure 3b, $p=0.007$), it appeared that 2.5 MED had higher expression.

Discussion

Previously we reported that 4 MED of UV resulted in activation of proteins within the MAPK, PI3K, p53 and JNK pathways (12). In the current study we investigated the impact of a lower and more applicable dose of SSL on key proteins on MAPK signaling. We then expanded the work to assess the impact of acute low dose SSL on key proteins within the PI3K/Akt pathway, an essential pathway for which there are limited data with regard to the modulations that occur after both acute and chronic exposure to solar radiation.

Because skin is exposed to daily low dose UV over an individual's lifetime, the investigation of signaling pathway alterations that result from acute exposures of normal skin to SSL may have relevance to skin carcinogenesis. We expect to find both significant overlap, as well as significant differences, in the pathways that are modulated as a result of chronic solar light exposure (i.e., AK's and SCCs) compared to acute exposures. Although chronic exposure to sunlight is necessary to acquire the critical combination of gene mutations and altered cell signaling in skin for the development of UV-induced SCC, we propose that the study of acute effects of UV may serve as a model for investigation of the effects of SSL on this complex array of signal transduction pathways that are also likely involved in UV-induced carcinogenesis. The study of both acute and chronic solar light exposure may also serve as a model whereby critical signaling pathways and individual proteins can be identified as potential biomarkers for use as endpoints in clinical trials or as companion biomarkers. Furthermore, the study of both acute and chronic solar light exposure may allow for the development of interventions such as targeted therapies in a much shorter amount of time than required for studies using cancer as an endpoint.

Recently, our group (22) found cell-signaling derangements in SCC compared to AK or to normal skin using reverse phase protein microarray analysis (RPMA). We found statistically significant differences in protein expression within the MEK-ERKs and Akt/mTOR signaling pathways (22). Germane to the current study, we found phosphorylated forms of p38, ERK1/2, mTOR, p70S6K1, 4E-BP1, and histone H3 to be significantly increased in SCC compared to AK. P-4E-BP1 and p-Akt were also increased in AK compared to normal

skin (22). Chen et al (16) also showed that p-Akt (Serine473), p-mTOR (Serine2448), S6, and po-4E-BP1 (S65) were higher in SCC compared to AK.

Activation of the PI3K/Akt pathway is an important element in cell survival and proliferation after UV (14). In the current study, we show a small but significant increase in the phosphorylation of Akt (Serine473) at 5 hrs. Previous studies of Akt activation have primarily focused on UVB or UVA alone in keratinocytes or mouse skin with fewer human studies (11, 23–26). We next evaluated p-mTOR (Serine2448), a direct substrate of activated Akt, and found early and strong sustained activation. mTOR exists in two protein complexes: rapamycin-sensitive mTOR complex 1 (mTORC1) which is associated with phospho-mTOR (Serine2448) and the rapamycin-resistant mTOR complex 2 (mTORC2) which is associated with p-mTOR (Serine2481) (6, 27–29). Although there is limited information on the effect of UV on skin, both mTORC1 and mTORC2 are thought to play complementary roles in controlling proliferation and apoptosis after UVB-irradiation (6, 29).

p70S6K1 is a substrate of p-mTOR and when activated it phosphorylates its downstream target, S6 to initiate protein synthesis. In the current study, we observed a marked and sustained increase in p-S6 (Serine235/S236) expression. Studies have shown that UV-irradiation is associated with increased p70S6 kinase phosphorylation, but fewer studies have addressed the activation of S6 following UV-irradiation (25). The activity of p-4E-BP1, another downstream target of mTOR, is inhibited through its interaction with mTOR (7). 4E-BP1 is a translational repressor that negatively regulates the eukaryotic initiation factor, eIF-4 (30). We found that phosphorylation of 4E-BP1 at Threonines 37 and T46 was significantly increased 24 hrs. A limited number of studies have demonstrated activation of 4E-BP1 by UVB-irradiation (18, 30).

We next explored the effect of 2–3 MEDs of SSL on the MAPK signaling pathway. The MAPK family includes ERKs, JNKs, and p38 kinases (18). MAPK pathways are activated as a result of growth factors or stress such as UV-irradiation and have central roles in transducing extracellular signaling to intracellular target proteins involved in cell growth and proliferation (18). We previously reported that p-p38 was increased at 1 hr with a further increase at 24 hrs after 4 MEDs (12). In the current study, 2–3 MED of SSL resulted in peak phosphorylation between 1–5 hrs followed by a decrease at 24 hrs. Our results using 2–3 MED are more consistent with previous studies using *in vitro* models (mouse or human keratinocytes) and mouse epidermis where phosphorylation of p38 occurred within minutes post-UVB and returned to basal levels by 24 hrs (9, 31, 32).

In the current study, SSL-induced phosphorylation of ERK 1/2, another key MAPK protein, was observed to be immediate and sustained as previously shown with UVB (33). Activation of ERK1/2 in skin after UVA or B has been studied *in vitro* and in vivo using murine models with variable results {(18, 24, 25). In human epidermis, acute UVB activated ERK 1/2 within 30 mins and remained elevated for 24 hrs using 2 MED (33). We found that phosphorylation of histone H3 (Serine10) peaked at 5 hrs and was decreased at 24 hrs, post-SSL. Histone H3 is a core structural protein of the nucleosome and phosphorylation of histone H3 at Serine 10 is essential for immediate-early gene expression, chromatin remodeling, and chromosome condensation during mitosis (34). ERKs and p38 kinases are

mediators of UVB-induced histone H3 phosphorylation at Serine10 in mouse epidermal cells (35).

UVB-induced COX-2 expression has been shown to occur via activation of the p38 MAPK/MSK1 pathway, which in turn results in phosphorylation of histone H3 to stimulate COX-2 expression (9, 36). COX-2 is increased after UVA or UVB irradiation in human and murine skin (31, 37–40). Moreover, COX-2 expression is increased in SCCs and AK compared to normal skin (39). Increased COX-2 leads to increased PGE2, cell proliferation and tumor promotion (39). We previously reported (12) that 4 MED of UV resulted in increased COX-2 expression at 24 hrs, a finding confirmed in this current study. In addition, we found that COX-2 expression was increased as early as 5 hrs post SSL.

The p53 tumor suppressor gene plays an important role in UV-induced skin carcinogenesis (41). p53 is a highly regulated gene that plays a key role in skin homeostasis. p53 is normally present at low levels, but an insult such as UV-irradiation can lead to increased p53 protein stability and nuclear accumulation (18, 42). This increase in p53 stability and accumulation occurs as a result of UV-induced phosphorylation of p53 through MAPKs that include p38 and ERK. p53 is frequently mutated in cutaneous SCCs and AK and in addition p53 mutations are present in sun-exposed skin providing strong evidence that there is a field effect of UV-exposure on skin (43). In the current study, a significant increase in total p53 protein was observed at 5 hrs with maximal expression at 24 hrs. In a previous study we found that phospho-p53 (Serine15) was present at 24-hrs post 4 MED of UV (12). Activation or increased expression of p38, ERK 1/2, and p53 have been reported to dose-related and likely wavelength dependent (18, 44).

We also measured the effect of SSL on proliferation and apoptosis. PCNA expression was largely unchanged over 24 hrs with the exception of a small but significant reduction at 5 mins post SSL. As we have previously observed (12), apoptosis was significantly increased at 24-hrs post SSL (e.g. cleaved caspase 3 or morphologically apoptotic cells). In our previous study using 4 MED, levels of apoptosis were higher (12). The cellular reaction to UV-irradiation is complex and results in the stimulation of multiple cell signaling pathways. p53 responds to UV-induced DNA damage where cells that are too damaged for complete repair go on to apoptosis in an effort to eliminate severely damaged cells and reduce the risk of transforming mutations (45). Pathways such as the PI3K pathway push cells toward survival where activated Akt inhibits p53 and apoptosis, but there are other pathways that can stimulate or inhibit apoptosis following SSL (7, 14, 46). There are also p53-independent mechanisms for UV-induced cell death that respond to UV-generated reactive oxygen species. Ultimately, the balance of pathway activation or suppression will determine the fate of damaged cells (17).

Analyses of the effect of MED on biomarker expression are shown in Supplementary Data Figures 1–3. For 7 of the 12 endpoints, there was not a statistically significant difference in expression by MED level. Conversely, for p-S6, p-ERK 1/2, and p-histone H3 there was a statistically significant difference in expression by MED level. There was no attempt to make the groups comparable and the small sample size precludes drawing conclusions with regards to these difference in marker expression by MED applied.

To conclude, we confirm that there is significant overlap between the pathway modulations observed in normal skin after acute SSL to those observed in SCC and AK, which result from years of chronic exposure. We chose specific proteins/phosphoproteins based on prior experience using *in vitro* and *in vivo* models as well as from our previous protein array work that implicated these specific pathways as important in the transition of AK to SCC, as well as those reported in the literature to have relevance in UV-induced carcinogenesis. Our study adds to the understanding of how the PI3K/Akt and MAPK signaling pathways respond to physiologically relevant acute doses of SSL in sun-protected human skin. These findings are crucial to the design of future studies analyzing the activation of signaling networks and identification of molecular targets for intervention in high-risk groups, in settings of acute sunburns as well as chronic skin damage. Progress in our understanding of mechanisms by which normal skin cells respond to solar light is vital for the identification and development of mechanistic-based approaches for the prevention and control of skin tumors, a continuously expanding cancer problem with significant morbidity and economic impact in terms of healthcare costs.

Supplementary Material

Refer to Web version on PubMed Central for supplementary material.

Acknowledgments

Financial Support. National Cancer Institute grants CA027502 (Yira Bermudez, Steven P. Stratton, Clara Curiel-Lewandrowski, James Warneke, Chengcheng Hu, George T. Bowden, Sally E. Dickinson, Kathylynn Saboda, Christine A. Brooks, David S. Alberts, Janine G. Einspahr), CA023074 (All authors received grant), and CA023074S2 (Yira Bermudez)

We would like to thank Mary Krutzsch and Michael Yozwiak for assistance with measurement of IHC and image analysis.

References

1. Rogers HW, Weinstock MA, Harris AR, Hinckley MR, Feldman SR, Fleischer AB, et al. Incidence estimate of nonmelanoma skin cancer in the United States, 2006. Arch Dermatol. 2010; 146:283–7. [PubMed: 20231499]
2. Harris RB, Griffith K, Moon TE. Trends in the incidence of nonmelanoma skin cancers in southeastern Arizona, 1985–1996. Journal of the American Academy of Dermatology. 2001; 45:528–36. [PubMed: 11568742]
3. Joseph AK, Mark TL, Mueller C. The period prevalence and costs of treating nonmelanoma skin cancers in patients over 65 years of age covered by medicare. Dermatol Surg. 2001; 27:955–9. [PubMed: 11737130]
4. Guy GP Jr, Machlin SR, Ekwueme DU, Yabroff KR. Prevalence and costs of skin cancer treatment in the U.S., 2002–2006 and 2007–2011. American journal of preventive medicine. 2015; 48:183–7. [PubMed: 25442229]
5. Gasparro FP. Sunscreens, skin photobiology, and skin cancer: The need for UVA protection and evaluation of efficacy. Environ Health Persp. 2000; 108:71–78.
6. Carr TD, DiGiovanni J, Lynch CJ, Shantz LM. Inhibition of mTOR suppresses UVB-induced keratinocyte proliferation and survival. Cancer Prev Res (Phila). 2012; 5:1394–404. [PubMed: 23129577]
7. Cao C, Wan Y. Parameters of protection against ultraviolet radiation-induced skin cell damage. J Cell Physiol. 2009; 220:277–84. [PubMed: 19360745]

8. Krutmann J. Ultraviolet A radiation-induced biological effects in human skin: relevance for photoaging and photodermatosis. J Dermatol Sci. 2000; 23 (Suppl 1):S22–6. [PubMed: 10764987]
9. Bachelor MA, Silvers AL, Bowden GT. The role of p38 in UVA-induced cyclooxygenase-2 expression in the human keratinocyte cell line, HaCaT. Oncogene. 2002; 21:7092–99. [PubMed: 12370831]
10. Keum YS, Kim HG, Bode AM, Surh YJ, Dong Z. UVB-induced COX-2 expression requires histone H3 phosphorylation at Ser10 and Ser28. Oncogene. 2013; 32:444–52. [PubMed: 22391560]
11. Bowden GT. Prevention of non-melanoma skin cancer by targeting ultraviolet-B-light signalling. Nat Rev Cancer. 2004; 4:23–35. [PubMed: 14681688]
12. Einspahr JG, Bowden GT, Alberts DS, McKenzie N, Saboda K, Warneke J, et al. Cross-validation of murine UV signal transduction pathways in human skin. Photochemistry and Photobiology. 2008; 84:463–76. [PubMed: 18248498]
13. Liu KD, Yu DH, Cho YY, Bode AM, Ma WY, Yao K, et al. Sunlight UV-Induced Skin Cancer Relies upon Activation of the p38 alpha Signaling Pathway. Cancer Research. 2013; 73:2181–88. [PubMed: 23382047]
14. Lopez-Camarillo C, Ocampo EA, Casamichana ML, Perez-Plasencia C, Alvarez-Sanchez E, Marchat LA. Protein Kinases and Transcription Factors Activation in Response to UV-Radiation of Skin: Implications for Carcinogenesis. Int J Mol Sci. 2012; 13:142–72. [PubMed: 22312244]
15. Vander Haar E, Lee SI, Bandhakavi S, Griffin TJ, Kim DH. Insulin signalling to mTOR mediated by the Akt/PKB substrate PRAS40. Nat Cell Biol. 2007; 9:316–23. [PubMed: 17277771]
16. Chen SJ, Nakahara T, Takahara M, Kido M, Dugu L, Uchi H, et al. Activation of the mammalian target of rapamycin signalling pathway in epidermal tumours and its correlation with cyclin-dependent kinase 2. Br J Dermatol. 2009; 160:442–5. [PubMed: 19016696]
17. Strozyk E, Kulms D. The role of AKT/mTOR pathway in stress response to UV-irradiation: implication in skin carcinogenesis by regulation of apoptosis, autophagy and senescence. Int J Mol Sci. 2013; 14:15260–85. [PubMed: 23887651]
18. Bode AM, Dong Z. Mitogen-activated protein kinase activation in UV-induced signal transduction. Sci STKE. 2003; 2003:RE2. [PubMed: 12554854]
19. Meloche S, Pouyssegur J. The ERK1/2 mitogen-activated protein kinase pathway as a master regulator of the G1- to S-phase transition. Oncogene. 2007; 26:3227–39. [PubMed: 17496918]
20. Rubinfeld H, Seger R. The ERK cascade: a prototype of MAPK signaling. Mol Biotechnol. 2005; 31:151–74. [PubMed: 16170216]
21. Ravnbak MH. Objective determination of Fitzpatrick skin type. Danish medical bulletin. 2010; 57:B4153. [PubMed: 20682135]
22. Einspahr JG, Calvert V, Alberts DS, Curiel-Lewandrowski C, Warneke J, Krouse R, et al. Functional Protein Pathway Activation Mapping of the Progression of Normal Skin to Squamous Cell Carcinoma. Cancer Prev Res. 2012; 5:403–13.
23. Decraene D, Agostinis P, Bouillon R, Degreef H, Garmyn M. Insulin-like growth factor-1-mediated AKT activation postpones the onset of ultraviolet B-induced apoptosis, providing more time for cyclobutane thymine dimer removal in primary human keratinocytes. J Biol Chem. 2002; 277:32587–95. [PubMed: 12070137]
24. Gu M, Dhanalakshmi S, Mohan S, Singh RP, Agarwal R. Silibinin inhibits ultraviolet B radiation-induced mitogenic and survival signaling, and associated biological responses in SKH-1 mouse skin. Carcinogenesis. 2005; 26:1404–13. [PubMed: 15831527]
25. Syed DN, Afaq F, Mukhtar H. Differential activation of signaling pathways by UVA and UVB radiation in normal human epidermal keratinocytes. Photochem Photobiol. 2012; 88:1184–90. [PubMed: 22335604]
26. Butts BD, Kwei KA, Bowden GT, Briehl MM. Elevated basal reactive oxygen species and phospho-Akt in murine keratinocytes resistant to ultraviolet B-induced apoptosis. Mol Carcinog. 2003; 37:149–57. [PubMed: 12884366]
27. Fingar DC, Blenis J. Target of rapamycin (TOR): an integrator of nutrient and growth factor signals and coordinator of cell growth and cell cycle progression. Oncogene. 2004; 23:3151–71. [PubMed: 15094765]

28. Sarbassov DD, Guertin DA, Ali SM, Sabatini DM. Phosphorylation and regulation of Akt/PKB by the rictor-mTOR complex. Science. 2005; 307:1098–101. [PubMed: 15718470]
29. Copp J, Manning G, Hunter T. TORC-specific phosphorylation of mammalian target of rapamycin (mTOR): phospho-Ser2481 is a marker for intact mTOR signaling complex 2. Cancer Res. 2009; 69:1821–7. [PubMed: 19244117]
30. Liu G, Zhang Y, Bode AM, Ma WY, Dong Z. Phosphorylation of 4E-BP1 is mediated by the p38/MSK1 pathway in response to UVB irradiation. J Biol Chem. 2002; 277:8810–6. [PubMed: 11777913]
31. Bachelor MA, Cooper SJ, Sikorski ET, Bowden GT. Inhibition of p38 mitogen-activated protein kinase and phosphatidylinositol 3-kinase decreases UVB-induced activator protein-1 and cyclooxygenase-2 in a SKH-1 hairless mouse model. Molecular cancer research: MCR. 2005; 3:90–9. [PubMed: 15755875]
32. Kim AL, Labasi JM, Zhu Y, Tang X, McClure K, Gabel CA, et al. Role of p38 MAPK in UVB-induced inflammatory responses in the skin of SKH-1 hairless mice. J Invest Dermatol. 2005; 124:1318–25. [PubMed: 15955110]
33. Fisher GJ, Talwar HS, Lin J, Lin P, McPhillips F, Wang Z, et al. Retinoic acid inhibits induction of c-Jun protein by ultraviolet radiation that occurs subsequent to activation of mitogen-activated protein kinase pathways in human skin in vivo. J Clin Invest. 1998; 101:1432–40. [PubMed: 9502786]
34. Nowak SJ, Corces VG. Phosphorylation of histone H3: a balancing act between chromosome condensation and transcriptional activation. Trends Genet. 2004; 20:214–20. [PubMed: 15041176]
35. Zhong SP, Ma WY, Dong Z. ERKs and p38 kinases mediate ultraviolet B-induced phosphorylation of histone H3 at serine 10. J Biol Chem. 2000; 275:20980–4. [PubMed: 10806218]
36. Perez-Cadahia B, Drobic B, Davie JR. H3 phosphorylation: dual role in mitosis and interphase. Biochem Cell Biol. 2009; 87:695–709. [PubMed: 19898522]
37. Bachelor MA, Bowden GT. UVA-mediated activation of signaling pathways involved in skin tumor promotion and progression. Seminars in Cancer Biology. 2004; 14:131–38. [PubMed: 15018897]
38. Buckman SY, Gresham A, Hale P, Hruza G, Anast J, Masferrer J, et al. COX-2 expression is induced by UVB exposure in human skin: implications for the development of skin cancer. Carcinogenesis. 1998; 19:723–9. [PubMed: 9635856]
39. An KP, Athar M, Tang X, Katiyar SK, Russo J, Beech J, et al. Cyclooxygenase-2 expression in murine and human nonmelanoma skin cancers: implications for therapeutic approaches. Photochem Photobiol. 2002; 76:73–80. [PubMed: 12126310]
40. Chen W, Tang Q, Gonzales MS, Bowden GT. Role of p38 MAP kinases and ERK in mediating ultraviolet-B induced cyclooxygenase-2 gene expression in human keratinocytes. Oncogene. 2001; 20:3921–6. [PubMed: 11439356]
41. Sarasin A, Giglia-Mari G. p53 gene mutations in human skin cancers. Exp Dermatol. 2002; 11 (Suppl 1):44–7. [PubMed: 12444960]
42. Friedman PN, Kern SE, Vogelstein B, Prives C. Wild-type, but not mutant, human p53 proteins inhibit the replication activities of simian virus 40 large tumor antigen. Proc Natl Acad Sci U S A. 1990; 87:9275–9. [PubMed: 2174557]
43. Ratushny V, Gober MD, Hick R, Ridky TW, Seykora JT. From keratinocyte to cancer: the pathogenesis and modeling of cutaneous squamous cell carcinoma. J Clin Invest. 2012; 122:464–72. [PubMed: 22293185]
44. Pfundt R, van Vlijmen-Willems I, Bergers M, Wingens M, Cloin W, Schalkwijk J. In situ demonstration of phosphorylated c-jun and p38 MAP kinase in epidermal keratinocytes following ultraviolet B irradiation of human skin. J Pathol. 2001; 193:248–55. [PubMed: 11180173]
45. Ziegler A, Jonason AS, Leffell DJ, Simon JA, Sharma HW, Kimmelman J, et al. Sunburn and p53 in the onset of skin cancer. Nature. 1994; 372:773–6. [PubMed: 7997263]
46. Wan YS, Wang ZQ, Shao Y, Voorhees JJ, Fisher GJ. Ultraviolet irradiation activates PI 3-kinase/AKT survival pathway via EGF receptors in human skin in vivo. Int J Oncol. 2001; 18:461–6. [PubMed: 11179472]

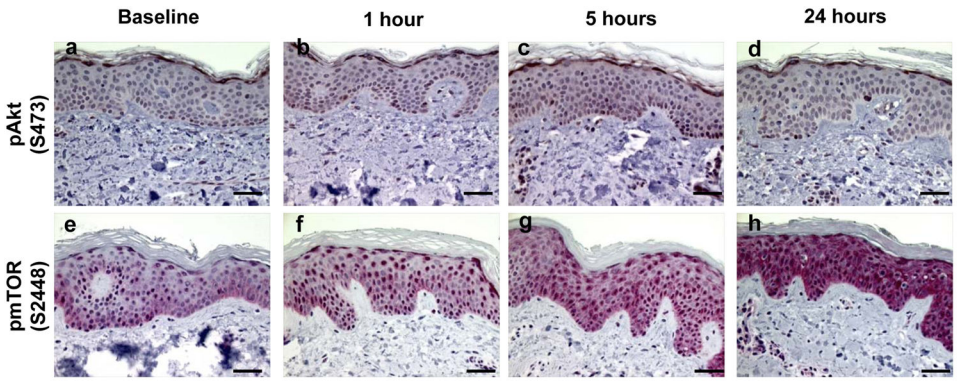

Figure 1.

Examples of immunohistochemically stained proteins in sun-protected skin after 2–3 MED of SSL-irradiation. Phospho-Akt (Serine 473), at baseline (a), 1 hour (b), 5 hours (c), and 24 hours (d). Phospho-mTOR (Serine 2448) expression at baseline (e), 1 hour (f), 5 hours (g), and 24 hours (h). Images are at a magnification of 400X and the scale bar represents 50 μm. Red nuclear and cytoplasmic staining is positive and blue is negative.

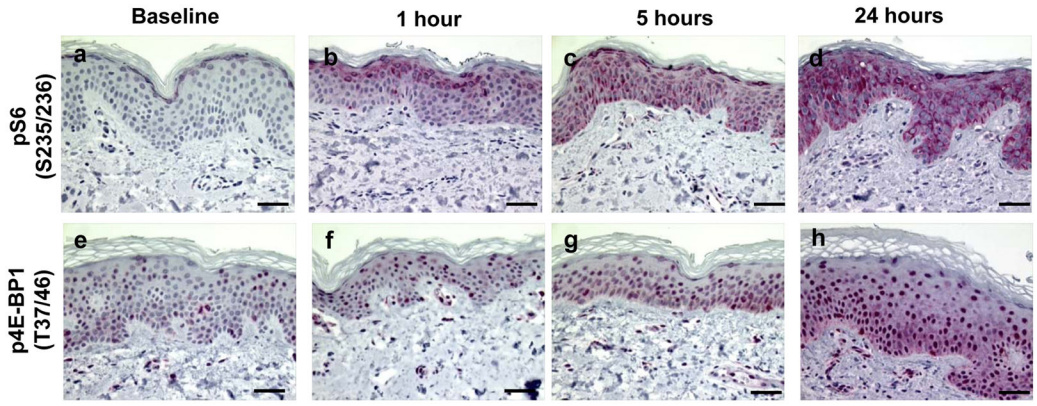

Figure 2.

Examples of immunohistochemically stained proteins in sun-protected skin after 2–3 MED of SSL-irradiation. Phospho-S6 (Serines 235/236) expression at baseline (a), 1 hour (b), 5 hours (c), and 24 hours (d). Phospho-4E-BP1 (Threonines 37/46) expression at baseline (e), 1 hour (f), 5 hours (g), and 24 hours (h). Images are at a magnification of 400X and the scale bar represents 50 μm. Red nuclear and cytoplasmic staining is positive and blue is negative.

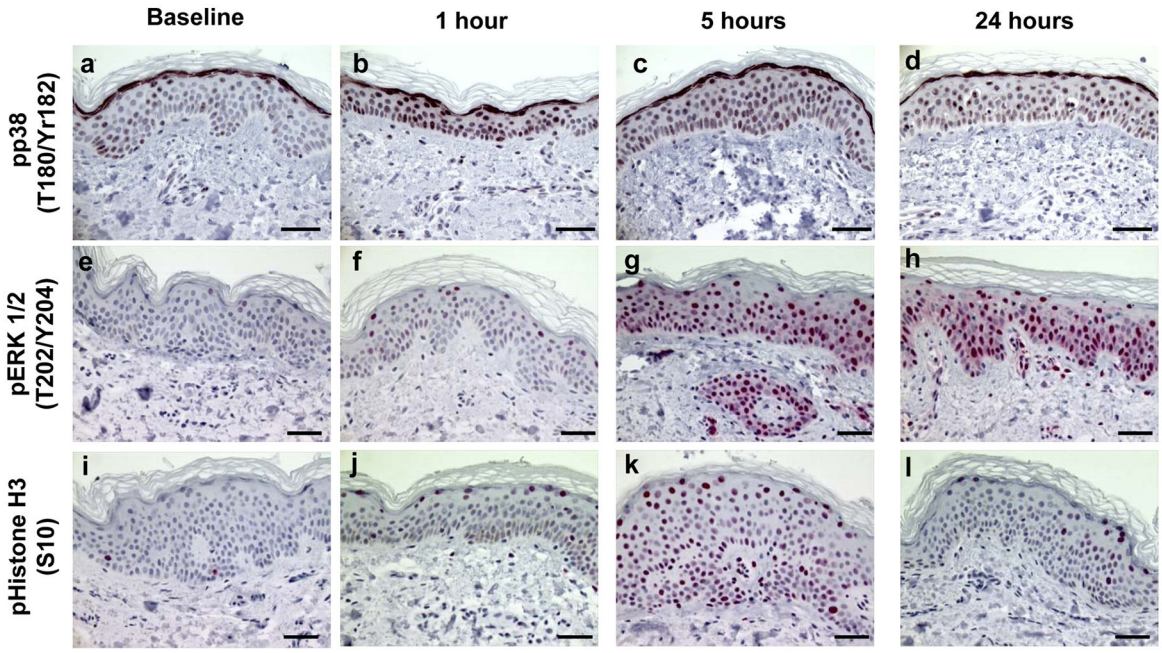

Figure 3.

Examples of immunohistochemically stained proteins in sun-protected skin after 2–3 MED of SSL-irradiation. Phospho-p38 (Threonine 180/Tyrosine 182) expression at baseline (a), 1 hour (b), 5 hours (c), and 24 hours (d). Phospho-ERK 1/2 (Threonine 202/Tyrosine 204) expression at baseline (e), 1 hour (f), 5 hours (g), and 24 hours (h). Phospho-histone H3 (Serine 10) expression at baseline (i), 1 hour (j), 5 hours (k), and 24 hours (l). Images are at a magnification of 400X and the scale bar represents 50 μm. Red (phospho-ERK 1/2 and phospho-histone H3) or brown (phospho-p38) nuclear and cytoplasmic stains represent positive and blue stain represents negative staining.

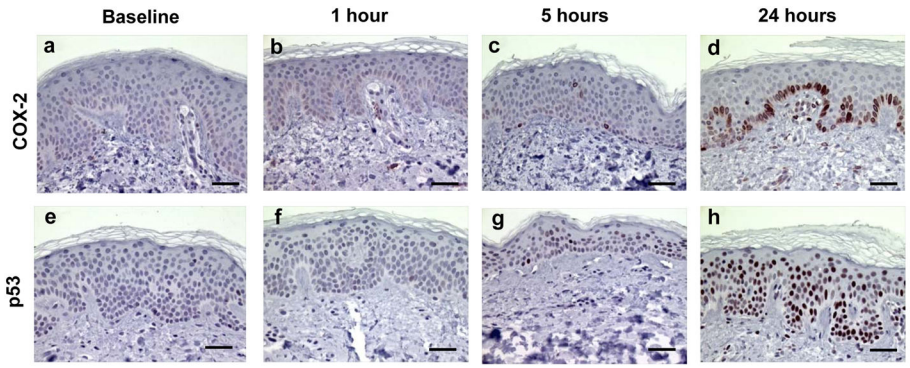

Figure 4.

Examples of immunohistochemically stained proteins in sun-protected skin after 2–3 MED of SSL-irradiation. COX-2 expression at baseline (a), 1 hour (b), 5 hours (c), and 24 hours (d). p53 expression at baseline (e), 1 hour (f), 5 hours (g), and 24 hours (h). Images are at a magnification of 400X and the scale bar represents 50 μm. Brown nuclear and cytoplasmic stains represent positive and blue stain represents negative staining.

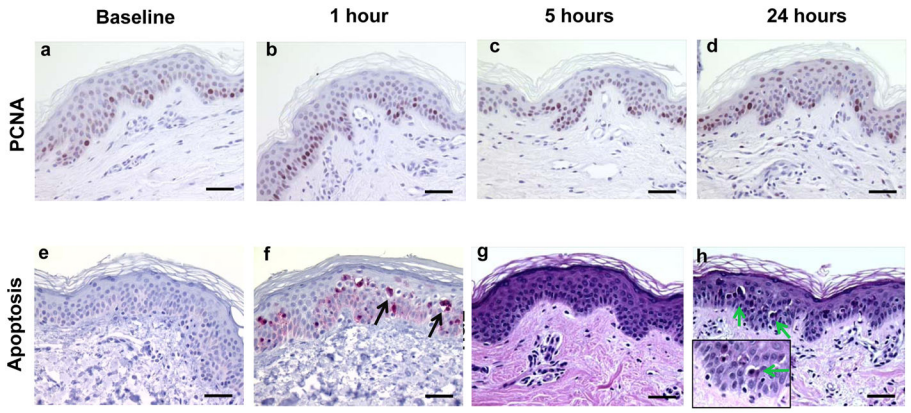

Figure 5.

Examples of proliferation and apoptosis in sun-protected skin after 2–3 MED of SSL-irradiation. PCNA expression at baseline (a), 1 hour (b), 5 hours (c), and 24 hours (d) post SSL. Cleaved caspase 3 at baseline (a) and 24 hours (b). Apoptotic cells on H&E stained slides at baseline (c) and at 24 hours with inset in the lower left at a magnification of 1000X (d). Images of are at a magnification of 400X the scale bar represents 50 μm. Brown nuclear stain is positive for PCNA (a–d). Red stain is positive and blue is negative for cleaved caspase 3 (e and f). Arrows point to apoptotic cells present at 24 hours post SSL.

Table 1

Means ± Standard of Error for Markers*

Biomarker	N	Baseline	5 minutes	p-value[1]	1 hour	p-value[1]	5 hours	p-value[1]	24 hours	p-value[1]	Time Trend p-value
p-Akt[4]	24	12.3±2.0	10.8±1.7	0.502	13.9±2.1	0.383	17.8±2.2	↑0.010	12.7±1.7	0.658	0.108
p-mTOR[4]	24	21.4±4.3	23.2±3.9	0.340	36.0±6.0	↑0.020	46.7±5.9	↑<0.0001	68.2±5.5	↑<0.0001	↑<0.0001
p-4E-BP1[4]	24	23.9±4.2	30.6±4.4	0.075	29.1±4.7	0.092	28.7±4.2	0.177	49.2±4.7	↑<0.0001	↑<0.0001
p-S6[2,4]	24	4.9±1.1	4.7±1.1	0.519	14.0±3.1	↑<0.0001	35.7±5.8	↑<0.0001	50.7±5.0	↑<0.0001	↑<0.0001
p-p38[4]	24	7.0±1.1	7.4±1.1	0.663	18.3±1.7	↑<0.0001	18.7±2.4	↑<0.0001	14.8±2.1	↑<0.0001	↑<0.0001
p-ERK 1/2[2,3]	24	4.2±1.0	6.0±1.3	↑0.012	16.0±4.7	↑0.004	22.0±4.1	↑<0.0001	23.8±3.3	↑<0.0001	↑<0.0001
p-histone H3[2,3]	24	1.5±0.4	2.2±0.7	0.816	8.4±2.0	↑<0.0001	29.5±5.7	↑<0.0001	9.1±2.3	↑<0.0001	↑<0.0001
COX-2[3]	24	0.3±0.1	0.1±0.03	0.116	0.4±0.2	0.590	2.0±0.3	↑<0.0001	17.1±1.4	↑<0.0001	↑<0.0001
p53[3]	22	1.3±0.3	1.4±0.4	0.837	1.1±0.3	0.844	4.5±1.2	↑<0.0001	26.1±2.8	↑<0.0001	↑<0.0001
PCNA[4]	24	25.6±2.5	20.8±2.2	↓0.023	26.2±3.4	0.930	30.1±3.3	0.214	21.0±2.2	0.114	0.832
Cleaved Caspase 3[2,3]	22	0.0±0.00	0.05±0.04	0.103	0.0±0.00	0.973	0.04±0.03	0.111	4.15±1.14	↑<0.0001	↑<0.0001
Morphologic Apoptosis	24	0.09±0.02	0.04±0.06	↓0.016	0.02±0.04	↓<0.0001	0.24±0.25	↑0.011	10.4±6.9	↑<0.0001	↑<0.0001

[1] p-values are for the difference between baseline and each time point.

[2] MED was controlled for in model.

[3] Ranks were used in the model.

[4] $y=\sqrt{x}$

* Arrows before p-values show the direction of change.